Dyes and Pigments 138 (2017) 68–76

Contents lists available at ScienceDirect

Dyes and Pigments

journal homepage: www.elsevier.com/locate/dyepig

On the design of a versatile ionic liquid, AOBH-DEHP, which can be used as a new molecular probe to investigate supramolecular assemblies

Matías A. Crosio, Juana J. Silber, R. Darío Falcone, N. Mariano Correa*

Departamento de Química, Universidad Nacional de Río Cuarto, Agencia Postal # 3, C.P. X5804BYA Río Cuarto, Argentina

ARTICLE INFO

Article history:
Received 5 September 2016
Accepted 20 November 2016
Available online 21 November 2016

Keywords:
Acridine orange
Protic ionic liquid
AOT

ABSTRACT

The motivation of our work is to find an exciting new molecular probe, which has the advantages that contains the acridine orange moiety but also has an ample range of solubility in different media. The probe is obtained through the acid-base reaction between acridine orange base (AOB) and bis-(2-ethylhexyl) phosphoric acid (HDEHP) giving AOBH-DEHP. This synthesized dye results to be a protic ionic liquid, since it is a viscous liquid at room temperature and, it is only constituted by ions.

The spectroscopic behavior of AOBH-DEHP in homogeneous medium, using water, benzene and *n*-heptane as solvents and, in benzene or *n*-heptane/sodium 1,4-bis-2-ethylhexylsulfosuccinate (AOT)/water reverse micelles (RMs) has been investigated. Absorption, emission and single photon counting techniques, were used to fully characterize the new molecule in different environments.

It is shown that AOBH-DEHP has all the advantages of its chromophore, $AOBH^+$ but, the presence of the hydrophobic anion, $DEHP^-$, gives to the dye, unique solubility in solvents of very different polarities. As such and, in contrast to $AOBH^+$ chloride salts, AOBH-DEHP can be used to determine different properties, such as micropolarity, restricted motion environment, critical micellar concentration in different RMs media.

1. Introduction

Organized systems are supramolecular assemblies characterized by the existence of a certain order of the entities that form them. The term “supramolecular” makes reference to those structures that involve molecular and ionic additives, which are held together by non-covalent interactions, such as electrostatic, hydrogen bond, dispersion forces and hydrophobic effects [1].

In contrast to ordinary solutions, where solute and solvent form a homogeneous phase at a molecular level, the organized solutions are characterized by being microscopically heterogeneous [1–4]. The organized systems that have sparked a higher interest during these last times are the reverse micelles (RMs). In them, the surfactant molecules have their polar head groups oriented inwards, while their hydrocarbonated tails are oriented outwards, where the non-polar solvent is located. Three specific environments can be found: the polar core, the micellar interface and the external organic phase [5,6]. In this way, these systems are adequate media for processes that imply hydrophilic and hydrophobic reactants, because they can be considered as “nano-reactors” for a variety of chemical and biological reactions [7–13].

In this sense, probably the best characterized system is the one formed by the ternary system non-polar solvent/sodium 1,4-bis-2-ethylhexylsulfosuccinate (Scheme 1) (AOT)/water [5,6,14–22]. The structure of the water in RMs media has been a topic of debate by many scientific researchers, most of whom assume that water molecules adopt two or more clear structures in the micellar interior [5,23–25]. The simplest approximation postulates two different structures of water; “united” and “free”, the first corresponding to water that is close to the headgroup and the counterions, at the interface, and the second one corresponding to water molecules that have more bulk solvent characteristics, and is set far from the RMs interface. The water properties (viscosity, polarity, hydrogen bonding capacity etc.) of the core (free) and the interfacial water vary with the water content and measured by W_o ($W_o = [H_2O]/[AOT]$) [5,26,27].

One of the many approaches to investigate the microenvironment of RMs media, is the use of spectroscopic techniques and

* Corresponding author.
E-mail address: mcorrea@exa.unrc.edu.ar (N.M. Correa).

http://dx.doi.org/10.1016/j.dyepig.2016.11.031
0143-7208/

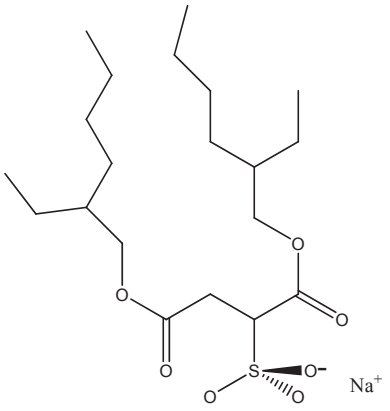

Scheme 1. Molecular structure of AOT.

molecular probes. When using optical probe, in order to provide useful information, it is expected that they do not perturb the system under investigation, that they have the proper location within the RMs and, are sensitive enough to the changes in its microenvironment [14]. Different compounds have been used as molecular probes for micellar systems [5,17,21,28,29]. One of them is acridine orange (Scheme 2) which is a cationic-basic fluorescent dye. In its basic form (AOB), is a proton acceptor and consequently can penetrate into the membrane of some cells accepting protons. However, the cationic molecule ($AOBH^+$) is not able to do so and therefore remains within the cell and could cause a variation in the ion local concentration [30]. Studies on $AOBH^+$ behavior in aqueous solution and its interaction with synthetic and biological systems have been the subject of interest for more than 50 years [31].

$AOBH^+$ is a very useful model for self-associating systems. Its monomer-dimer behavior was reported in microemulsion media [32,33]. It was found that in compartmentalized environments such as decane or *n*-heptane/AOT/water RMs the dimerization is reduced, and this have a potential application for the preparation of dye lasers, which require a noninteracting monomeric form of the dye [32].

Previous studies of the spectroscopic behavior of AOB in AOT RMs show that includes different process, such as acid-base and dimerization equilibria which vary with the conditions used [7,34]. It was shown that AOB enters the AOT RM interface only if it is protonated to give $AOBH^+$, which is not soluble in the organic pseudophase. By varying the AOT concentration it is possible to control the dimerization process of $AOBH^+$ having the monomer or the dimer depending on the occupation number value [7]. Thus, the use of AOB as molecular probe to monitor micellization processes is not convenient in aqueous RMs, since its spectroscopic behavior is very complex. On the other hand, it was demonstrated that it is useful to determinate RMs properties in non-aqueous AOT RMs, where the protonation equilibrium is not possible [34].

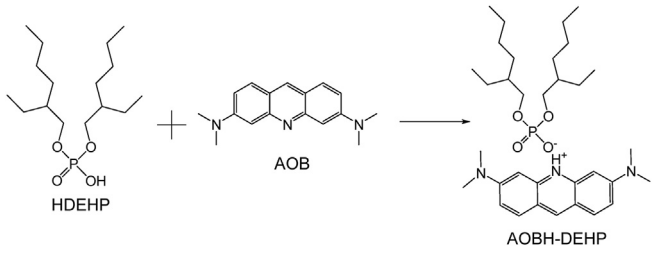

Scheme 2. Synthesis of AOBH-DEHP.

On the other hand, since $AOBH^+$ molecule, as it was mentioned above, is not soluble in non-polar organic solvents, its application as a molecular probe to monitor the micellization process of RMs is not encouraged since it will dissolve only when the RMs is already formed. However, when the organized system is present this probe is useful for studying properties such as micropolarity, critical micelle concentration (cmc) among others [7,32,33]. In this sense, it seems quite interesting to find a new molecular probe that has all the advantages of the $AOBH^+$ molecule but soluble in most of the organic solvents.

Ionic liquids (ILs) have received significant attention as powerful alternatives to conventional molecular organic solvents [35–37]. According to their proton availability, ILs can be classified as protic or aprotic [38]. Particularly, protic ILs (PILs) have been used in several applications [35,39]. PLIs are molten salt at room temperature, which are obtained by an acid-base reaction [16,40].

In this work we present results on a new PIL, AOBH-DEHP, which is formed by the acid-base reaction between AOB and bis-(2-ethylhexyl) phosphoric acid (HDEHP), as shown in Scheme 2. Such molecule was thought with the goal of obtaining a molecule with more amphiphilic character than $AOBH^+$, due to the long hydrocarbon chain of the anion DEHP [21,41]. This comes out since it was demonstrated that surfactant sodium bis-(2-ethylhexyl) phosphate (NaDEHP) forms aqueous and non-aqueous RMs showing the amphiphilic nature of the anion DEHP [41].

The results show that AOBH-DEHP is very promising for monitoring the properties of RMs formed in different non-polar solvents. Thus, very well-known AOT RMs, namely *n*-heptane or benzene/AOT/water systems as well as bulk *n*-heptane, benzene and water, were investigated in order to assess the potential that the new PIL has as molecular probe.

2. Materials and methods

2.1. Materials

The surfactant sodium 1,4-bis-2-ethylhexylsulfosuccinate (AOT) (Sigma >99% purity) was used as received and it was kept under vacuum to avoid water absorption. The surfactant was kept under vacuum in order to minimize water absorption.

The used solvents (*n*-heptane, benzene and water) were of HPLC quality (Sigma-Aldrich and Sintorgan), and were used as received.

Acridine orange base (AOB) dye, Sigma 95% purity, and the surfactant bis-(2-ethylhexyl) phosphoric acid (HDEHP), Fluka 95% purity, were used as received.

Synthesis of AOBH-DEHP: The synthesis was carried out through the acid-base reaction between AOB and HDEHP as shown in Scheme 2. 5×10^{-3} mol of AOB with 7×10^{-3} mol of HDEHP were mixed. The amounts were calculated in a way that HDEHP is slightly exceeding, to assure that the AOB reacted completely. Both reactants were mixed without solvent and left to react during 24 h with constant agitation at room temperature. When the reaction time has passed, the HDEP acid excess was evaporated at room temperature and reduced pressure (in a rotary evaporator). As a result, the AOBH-DEHP molecule was obtained which has an appearance of a reddish viscous liquid.

2.2. Methods

A stock solution of AOBH-DEHP was prepared at a concentration of 1×10^{-3} M in methanol. Then the appropriate amount of this solution was transferred to a volumetric flask to obtain a concentration of 1×10^{-5} M in the micellar system, and the methanol was evaporated by bubbling off dry N_2.

Benzene/AOT or *n*-heptane/AOT RMs solutions were prepared

by weighing and dilution. In order to obtain optically transparent solutions, they were agitated in a sonication bath. In all the experiments, stock solutions of 3×10^{-1} M for AOT were prepared in the corresponding solvent (benzene or *n*-heptane depending on the system). These stock solutions were diluted to obtain different AOT concentrations.

When working with neat *n*-heptane, and to increase the polarity of the medium and therefore facilitate the whole dissolution of AOBH-DEHP, it was always added a minimum amount of AOT concentration of 5×10^{-5} M, far below the cmc value of this surfactant [5].

Water addition was carried using a calibrated microsyringe. The water content in the system is expressed, as the molar ratio between water and surfactant ($W_0 = [H_2O]/[surfactant]$).

In *n*-heptane/AOT RMs studies, the variation of the surfactant concentration was performed at two W_0 values (0 and 10). The $W_0 = 0$ corresponds to a system without the addition of water, but with the presence of residual water corresponding to the intrinsic humidity of the media ($W_0 \sim 0.3$) [42].

For studies varying the W_0 values and, for the Red-Edge Excitation Shift (REES) experiments, a surfactant concentration of about 3×10^{-1} M was used.

2.3. General

The absorption experiences were made in a Shimadzu equipment 2401 at 25.0 ± 0.1 °C. The optical path used in the absorption experiments was of 1 cm. A Spex Fluoromax spectroflourometer was used for the fluorescence measurements. The corrected fluorescence spectra were obtained using the correction file provided by the manufacturer. The emission spectra in benzene and water, since the emission intensity in these media is high, were taken in a triangular cell to avoid auto quenching effect, while in *n*-heptane a regular optical path cell was used.

Fluorescence decay data were measured with the time correlated single photon counting technique (TCSPC) (Edinburgh Instrument FL-900) with a PicoQuant sub-nanosecond FL-900 LED excitation at 460 and 495 nm. The quality of the fits was determined by the reduced χ [2] that must be around 1.0 [43].

Emission decays were interpreted using the lifetime's distribution analysis software provided by Edinburgh Instruments (i.e. the EI method). Details of the algorithm used by the EI method to find the lifetime's distribution that best fits the experimental decays has been discussed elsewhere [44–46].

3. Results and discussion

Firstly, it was performed a detailed investigation of the photophysical behavior of the dye in a homogeneous medium. Thus, the variation of the concentration of AOBH-DEHP between 9×10^{-6} M to 1×10^{-4} M, in water, benzene and *n*-heptane was performed. As it was pointed out, a minimum concentration of AOT equal to 5×10^{-5} M is needed in *n*-heptane, to increase the polarity of the medium and, therefore allowing the dye's dissolution.

The RMs studied were benzene/AOT/water and *n*-heptane/AOT/water. The experiments in the RMs media consisted in varying the concentration of the surfactant and the water content (W_o) and, the solvatochromic behavior of the dye was monitored by absorption and fluorescence techniques.

3.1. Homogeneous medium

3.1.1. Water

Fig. 1 A shows the absorption spectra varying the concentration of AOBH-DEHP in water. Two bands can be observed with maxima at λ = 468 nm and a shoulder at λ = 491 nm, which do not obey Lambert-Beer's law (Figure S1 A) These facts might be telling us

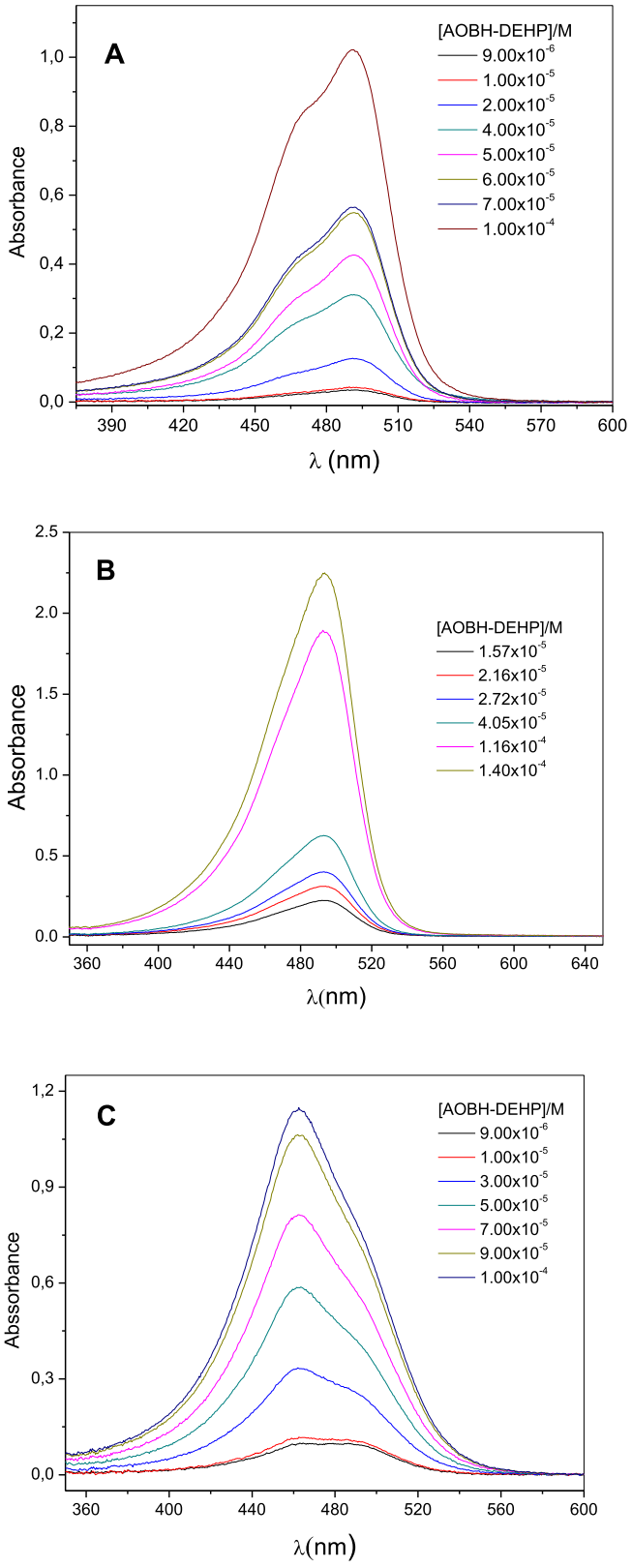

Fig. 1. Absorption spectra varying the concentrations of AOBH-DEHP between 9×10^{-6} M and 1×10^{-4} M. **A**: in water. **B**: in benzene **C**: in *n*-heptane. $[AOT] = 5 \times 10^{-5}$ M.

that there is more than one species present in this medium, probably because the molecule undergoes an aggregation process [7]. As it was determined for $AOBH^+$ in water, the band at $\lambda = 491$ nm is assigned to the monomer species while the one at $\lambda = 468$ nm is assigned to the aggregated species [7,20].

The emission spectra of AOBH-DEHP in water at $\lambda_{exc} = 490$ nm is shown in the Supplementary Information section as Fig. S1 B. The plot shows a unique emission band with a maximum at $\lambda = 532$ nm. When the emission spectra is obtained exciting at the absorption's maximum of the aggregate ($\lambda = 468$ nm) also shows one emission band at $\lambda = 532$ nm corresponding, in both cases, to the emission of the monomer species. The emission of the aggregate is not detected, in contrast to the emission observed for $AOBH^+$ in water where the dimer species emits at $\lambda = 650$ nm [7]. Since the anion DEHP (Scheme 2) is highly hydrophobic, it seems that in order to be dissolved in water AOBH-DEHP needs to form aggregates.

3.1.2. Benzene

Fig. 1B shows the spectra of the molecule AOBH-DEHP varying the concentration in benzene. In contrast to what it was observed in water, the spectra show a unique absorption band, with a maximum at $\lambda = 499$ nm, which obey Lambert-Beer's law through the whole range of concentration used (result not shown).

In the emission spectra of AOBH-DEHP excited at the absorption's band maximum ($\lambda = 499$ nm) only one emission band is observed with an emission maximum at $\lambda = 533$ nm (result not shown). We can conclude that, in benzene there is only one species of AOBH-DEHP present, the monomer.

3.1.3. n-heptane

Fig. 1C shows the absorption spectra varying the concentration of AOBH-DEHP in *n*-heptane. Two absorption bands with the maxima at $\lambda = 462$ nm and $\lambda = 488$ nm, which do not obey the Lambert-Beer's law, are observed (not shown). At low concentrations of AOBH-DEHP both bands have the same intensity. As the AOBH-DEHP concentration increases, the band at $\lambda = 462$ nm becomes the main band with a shoulder at $\lambda = 488$ nm. These results indicate that there is more than one species present in this medium, which means that the molecule AOBH-DEHP is aggregating. As it was assigned earlier, a monomer peaks at $\lambda = 488$ nm and the aggregated species at $\lambda = 462$ nm.

Fig. S2A shows the emission spectra of AOBH-DEHP exciting at $\lambda = 488$ nm, the absorption maximum corresponding to the monomer. As it can be observed, one emission band is observed at $\lambda = 532$ nm, as the concentration of AOBH-DEHP increases. Furthermore, there is no change in the spectra shape and, only an increase in the intensity and a shift to the red is detected. On the other hand, when the molecule is excited at the absorption maxima that corresponds to the aggregated species, $\lambda = 462$ nm (Fig. S2B), aside from the emission band at $\lambda = 532$ nm a shoulder is observed around 611 nm. This shoulder could be the emission from the aggregated species which is characteristic of the $AOBH^+$ dimer [7,30–33]. Thus, we assume that most of this aggregate could be a dimer, as we confirmed with lifetimes distribution analysis (see below).

3.2. Reverse micellar media

3.2.1. Benzene/AOT/water

Fig. S3A shows the absorption spectra of AOBH-DEHP by varying the AOT concentration in the RM system benzene/AOT at $W_0 = 0$, at AOBH-DEHP concentration of 1×10^{-5} M. Only one absorption band can be observed with a maximum at $\lambda = 499$ nm and, no changes were observed in the absorption spectra with the increase of the surfactant concentration.

Fig. S3B shows the emission spectra of AOBH-DEHP by varying the AOT concentration, when excited at $\lambda = 499$ nm. As it can be seen, a unique band is observed with a maximum at $\lambda = 534$ nm and, no changes are observed upon increasing the surfactant concentration.

Figs. S4A and B show the absorption and emission spectra of AOBH-DEHP by varying the AOT concentration but when water is added to the system, at $W_0 = 10$. As it was found without the water addition, there are no changes neither in the absorption nor in the emission spectra with the surfactant addition.

In both RMs media, without and with water, the absorption and emission maxima matches the values found in neat benzene (see Section 3.1.2). Thus, in this RMs the dye is exclusively located in the benzene pseudophase and it cannot be used to monitor RMs properties.

3.2.2. n-Heptane/AOT/Water

Fig. 2A shows the absorption spectra of AOBH-DEHP by varying the AOT concentration in the system *n*-heptane/AOT at $W_0 = 0$, at AOBH-DEHP concentration of 1×10^{-5} M. At [AOT] < cmc it is observed that there are two absorption bands; one of them with a maximum at $\lambda = 486$ nm corresponding to the monomer and the other one with a maximum at $\lambda = 466$ nm that we assign to the dimer, as it was observed in bulk *n*-heptane (see section 3.1.3). As the AOT concentration increases, the band with the maximum at $\lambda = 466$ nm disappears and the band with the maximum at $\lambda = 486$ nm develops as the main band, with a bathochromic shift to $\lambda = 496$ nm.

Fig. 2B shows the emission spectra of AOBH-DEHP when excited at $\lambda = 490$ nm (maximum absorption of the monomer) varying the surfactant concentration. At [AOT] < cmc the dye shows a band with a maximum at $\lambda_{emi} = 528$ nm. As the AOT concentration increases, the maximum of the emission band undergoes a bathochromic shift to $\lambda = 538$ nm with a notorious increase in the band intensity.

The addition of water to the system ($W_0 = 10$) is shown in Figs. S5, A and B for the absorption and emission spectra, respectively. It can be seen a similar behavior to the one observed without water addition. The absorption spectra shows two bands, one with a maximum at $\lambda = 488$ nm corresponding to the monomer, and the other one at $\lambda = 465$ nm corresponding to the dimer. At [AOT] > cmc, the band at $\lambda = 465$ nm disappears and the band at $\lambda = 488$ nm shifts to $\lambda = 494$ nm.

These results can be explained taking into account the disaggregation power that AOT RMs observed with other molecular probes [7,28,47]. By increasing the AOT concentration, the concentration of RMs, shown in equation (1) also increases.

$$[RM] = \frac{[AOT] - cmc}{N_{agg}} \quad (1)$$

where [RM] represents the concentration of RMs, with N_{agg} the aggregation number, that is the number of surfactant molecules in the RMs [48] and, cmc the critical micellar concentration.

Taken into account a Poisson statistics, the occupation number, n, which can be defined as the average number of molecular probe per micelle, can be defined as Equation (2) shows, for concentration above the cmc [28].

$$n = \frac{[AOBH - DEHP]}{[RM]} \quad (2)$$

If n is smaller than one, on the average fewer than one molecule probe occupies any given RM and, the predominant species will be the monomer. The opposite is valid for n larger than one. For *n*-

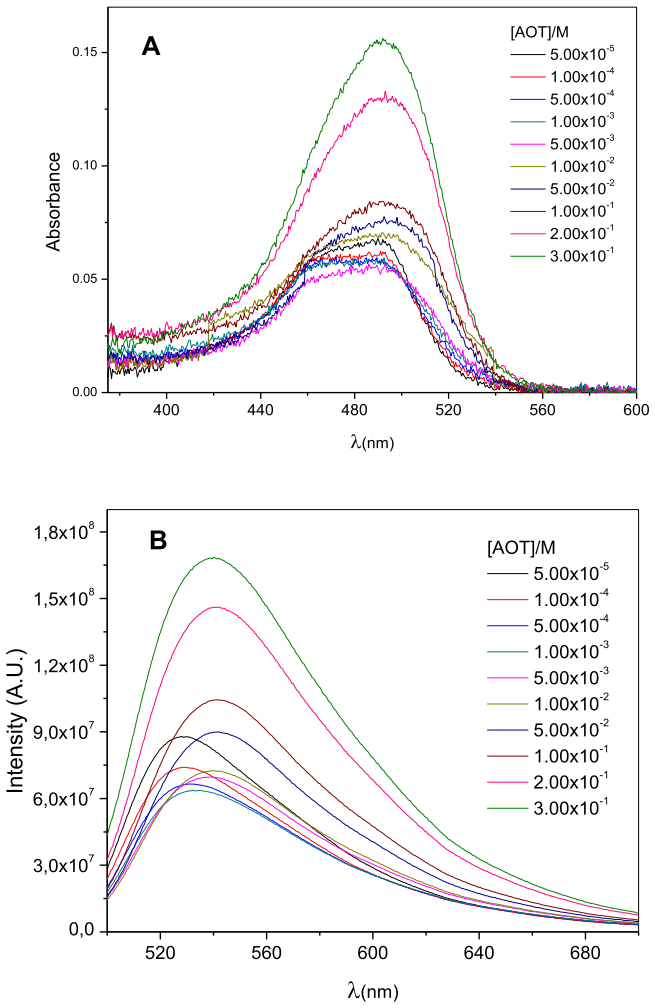

Fig. 2. A: Absorption spectra of AOBH-DEHP in *n*-heptane/AOT/water RMs at $W_0 = 0$ by varying the surfactant concentration. [AOBH-DEHP] $= 1 \times 10^{-5}$ M. **B**: Emission spectra of AOBH-DEHP in *n*-heptane/AOT/water RMs at $W_0 = 0$ by varying the surfactant concentration. [AOBH-DEHP] $= 1 \times 10^{-5}$ M $\lambda_{exc} = 490$ nm.

heptane/AOT/water RMs at $W_0 = 10$, $N_{agg} = 100$[48] and cmc $= 2 \times 10^{-4}$ M[14] and, the different [RM] and n values are gathered in Table 1, for the whole AOT concentration range used. It can be seen that for [AOT] $< 1 \times 10^{-3}$ M, n > 1 both species (dimer and monomer) are found in similar proportions For [AOT] $> 1 \times 10^{-3}$ M, n < 1 and the monomer species band increases at the expense of the dimer band. Therefore, at low n values, the probability of founding two AOBH-DEHP molecules in the same RMs is low and, the RMs environment leads almost to the complete disaggregation of the dye monomer.

Table 1
RMs Concentration and Occupation Number (n) for AOBH-DEHP in *n*-heptane/AOT/water at $W_0 = 10$ varying [AOT]. [AOBH-DEHP] $= 1 \times 10^{-5}$ M.

[AOT]/M	[RMs]/M	n
5×10^{-4}	3.00×10^{-6}	3.330
1×10^{-3}	8.00×10^{-6}	1.250
5×10^{-3}	4.80×10^{-5}	0.210
1×10^{-2}	9.80×10^{-5}	0.100
5×10^{-2}	4.98×10^{-4}	0.020
1×10^{-1}	9.98×10^{-4}	0.010
2×10^{-1}	1.99×10^{-3}	0.005
3×10^{-1}	2.99×10^{-3}	0.003

$N_{agg} = 100$ (ref 48) cmc $= 2 \times 10^{-4}$ M (ref 14).

3.2.2.1. Determination of the cmc. We use the ability that the AOT RMs has to disaggregate AOBH-DEHP dimer to determine the cmc value of the *n*-heptane/AOT/water RMs. Fig. 3, A and B show the plots of the dye absorbance at $\lambda = 488$ nm, corresponding to the monomer absorption, as a function of the log [AOT] at $W_0 = 0$ and 10, respectively. As it can be observed, the absorbance at $\lambda = 488$ nm abruptly increases at certain AOT concentration, that we assume is the cmc value. The cmc values were obtained from the crossing of the two straight lines. These values are $3.80 \pm 0.20 \times 10^{-3}$ M and $3.40 \pm 0.10 \times 10^{-4}$ M at $W_0 = 0$ and 10, respectively and match perfectly the data found in the bibliography for the same AOT RMs, within the range of experimental error [5]. In this way, we demonstrate that the new molecular probe, AOBH-DEHP is very useful to determine RMs properties such as the cmc value.

We also want to show other interesting features of AOBH-DEHP taking advantage of its chromophore, the cation $AOBH^+$. Thus, in the next section we describe what happens upon water addition, working at a concentration of surfactant where the dye exists mostly as monomer, namely [AOT] = 0.30 M.

3.2.3. Variation of the W_0

Fig. S6 A and B show the absorption and emission spectra of the dye ([AOBH-DEHP] $= 1 \times 10^{-5}$ M) at different W_0 values. Fig. S6 A

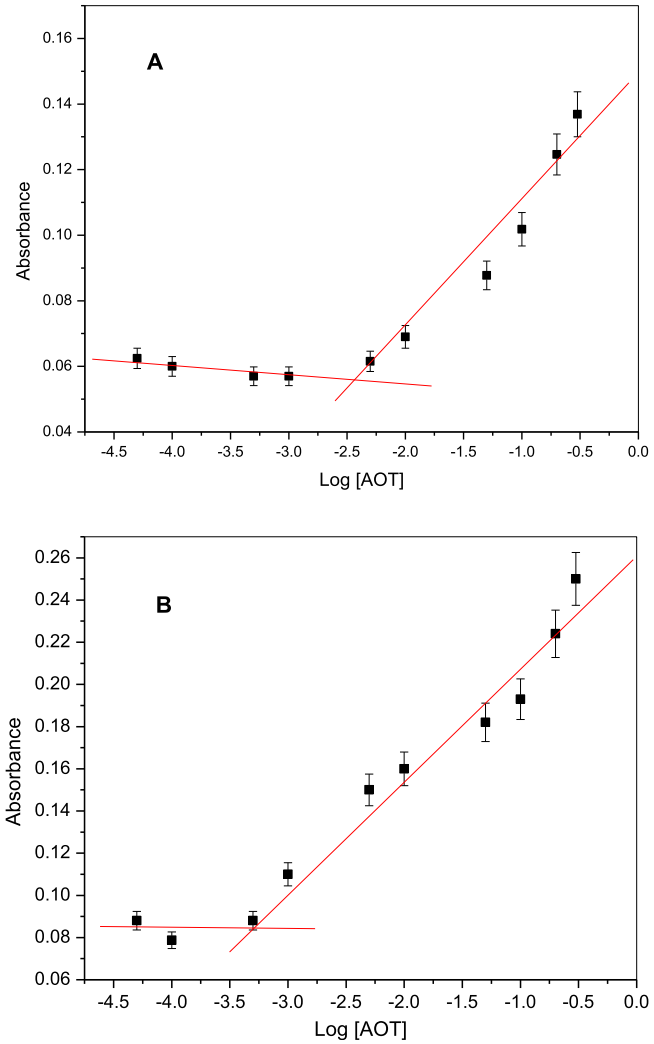

Fig. 3. Values of absorbance at $\lambda = 488$ nm vs. Log [AOT] in *n*-heptane/AOT/water RMs (**A**) $W_0 = 0$. (**B**) $W_0 = 10$. [AOBH-DEHP] $= 1 \times 10^{-5}$ M.

shows that, at $W_0 = 0$ the absorption spectra presents the band of the monomer and small shoulder at shorter wavelength corresponding to the dimer as described before. As the W_0 values increases, it can be seen that the band that peaks at $\lambda = 492$ nm increases at the expense of the band at $\lambda = 470$ nm. Therefore, the disaggregation phenomenon of AOBH-DEHP in *n*-heptane/AOT/water RMs is favored by the addition of water to the system.

Fig. S6 B shows that, at $W_0 = 0$ the emission maximum peaks at $\lambda = 537$ nm and, as the water content increases, the emission band intensity also increases and shifts bathochromically to a value of $\lambda = 547$ nm at $W_0 = 2$. For $W_0 > 4$ the emission band shifts hypsochromically to $\lambda = 538$ nm. Fig. 4 summarizes the changes in the position of the band with the water content. Previous studies have demonstrated that the molecule $AOBH^+$ in *n*-heptane/AOT/water RMs at low W_0 values, resides at the RMs interface. As the W_0 values increases, it moves to the water pool [7]. In the same way, AOBH-DEHP dissolved in AOT RMs can reside with the cation $AOBH^+$ located in the interface of the micelle at $W_0 = 0$. The bathochromic shift observed in the emission spectra, at low values of W_0, could be due to the fact that the molecule AOBH-DEHP at the interface, monitors the increasing in the micropolarity of the RMs interface upon water addition (Scheme 3A). On the other hand, when more water is added to the system, due to the hydrophobicity of the anion DEHP the whole dye moves into the surfactant tails, including the cation $AOBH^+$ which interacts strongly with the anion. Thus, the dye is in a less polar environment than the interface [5] (Scheme 3B) and the emission band shifts hypsochromically.

3.2.4. Red-edge excitation shifts (REES) in n-heptane/AOT/water RMs

It is known that, in solutions where the solvent relaxation is not complete around the fluorophore, the emission spectra maximum shifts to higher wavelengths when the excitation is at the red-edge of the absorption spectrum. This phenomenon is known as REES and is mainly observed in movement restricted media such as RMs [28,34,49–51].

For AOBH-DEHP the REES magnitude is characterized by the difference in the emission maximum when exciting at 530 nm and 490 nm according equation (3):

$$\text{REES} = \lambda_{em}\,(\text{excitation} = 530\ \text{nm}) - \lambda_{em}\,(\text{excitation} = 490\ \text{nm}) \quad (3)$$

Figs. S7, A and B, shows the emission spectra of AOBH-DEHP in AOT RMs at different excitation wavelength values, at $W_0 = 0$ and 10, respectively. As it can be observed, the band shifts bathochromically when the excitation wavelength is at the red-edge of the absorption spectra (Fig. 2A). This is consistent with the dye solubilized in the interior of the RMs revealing the constrained environment.

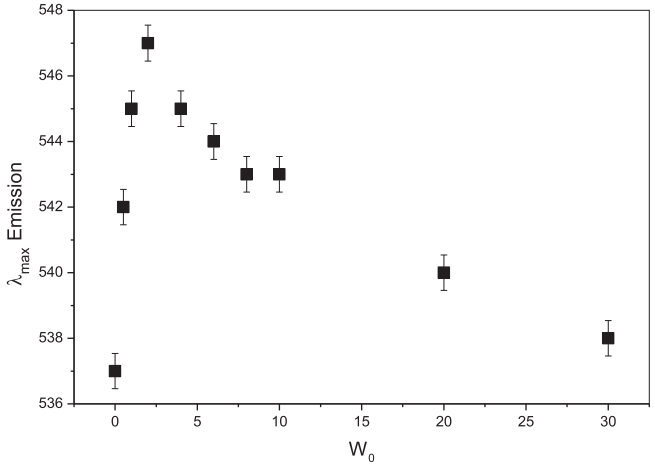

Fig. 4. Maximum emission wavelength dependence for AOBH-DEHP in *n*-heptane/AOT/water RMs with W_o. [AOT] = 0.30 M [AOBH-DEHP] = 1×10^{-5} M.

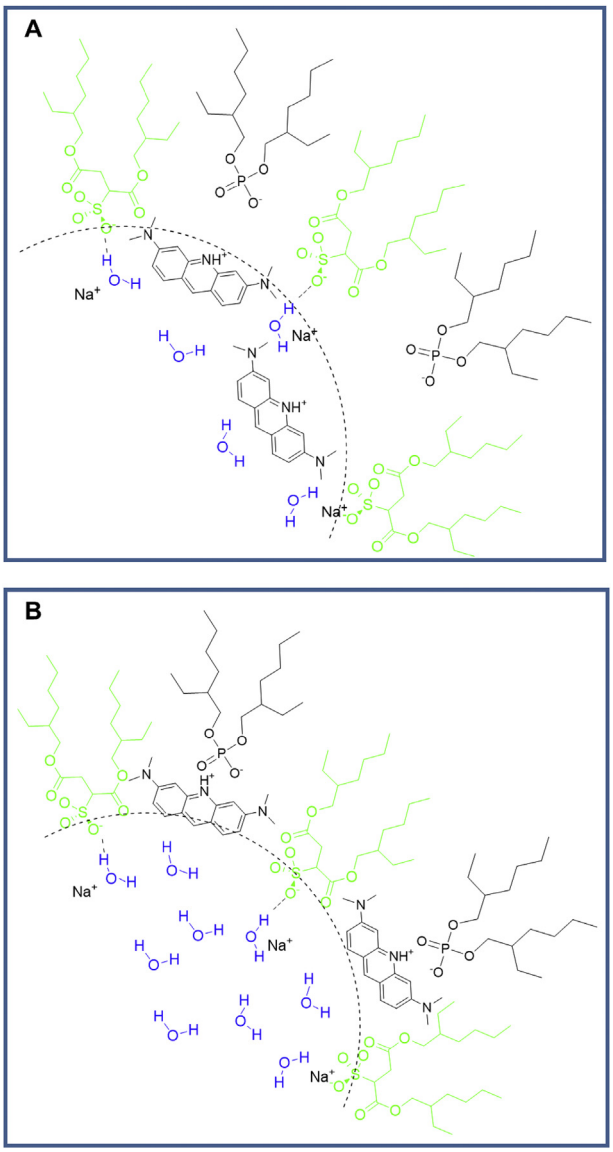

Scheme 3. Cartoon of the possible location of AOBH-DEHP at the AOT RMs interface. **A**: $W_0 < 4$ **B**: $W_0 > 4$.

Fig. 5 shows the REES magnitude as a function of W_0 values in *n*-heptane/AOT RMS at [AOT] = 0.3 M. As it can be observed, the REES value decreases suddenly from 9 nm at $W_0 = 0$ up to $W_0 = 1$ and, after that remains constant and equal to 3 nm. Thus, AOBH-DEHP not only shows what is already known for AOT RMs, that the addition of water makes the RMs interface more fluid and less viscous [5], but it also shows that as more water is added to the RMs, AOBH-DEHP moves to the oil side of the AOT RMs interface, embedded among the AOT hydrocarbon chains. An environment that it seems to be more fluid than the water side of the interface.

3.2.5. Lifetime distribution analysis

To get more insights on the characterization of the different

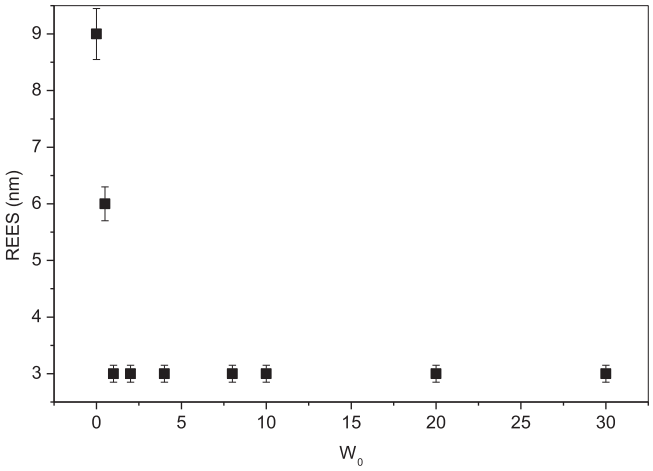

Fig. 5. REES Magnitude as a function of W_o for AOBH-DEHP in *n*-heptane/AOT/water RMs. [AOT] = 0.30 M [AOBH-DEHP] = 1×10^{-5} M.

species, lifetime distribution studies were conducted in homogeneous and, in AOT RMs media.

Table 2 shows the fluorescence lifetime values for AOBH-DEHP in water, benzene and *n*-heptane. In bulk water, the dye was excited at λ_{exc} = 460 nm and the emission monitored at two wavelengths: λ_{emi} = 527 nm and λ_{emi} = 610 nm. A single distribution was observed in both cases with an average lifetime of 1.67 ± 0.18 ns and 1.70 ± 0.10 ns, respectively. As it was not detected emission from the aggregate species, this lifetime was assigned to the monomer species. In bulk benzene, exciting at λ_{exc} = 460 nm and monitoring the emission at λ_{emi} = 533 nm, a single distribution was also observed with a lifetime of τ = 4.30 ± 0.60 ns. As AOBH-DEHP molecule in benzene exists as a monomer, this lifetime corresponds to this species. In bulk *n*-heptane, the distribution lifetimes values observed when it is excited at λ_{exc} = 495 nm and monitoring at λ_{emi} = 527 nm, correspond to a single distribution with a lifetime of τ = 4.60 ± 0.70 ns. On the other hand, when exciting at λ_{exc} = 460 nm and observing at λ_{em} = 610 nm, a bimodal distribution is obtained with the following lifetime values: τ = 4.00 ± 1.00 ns and τ = 15.10 ± 2.00 ns. In the first case (at λ_{exc} = 495 nm and λ_{emi} = 527 nm) the emission is from the monomer while, in the second case (λ_{exc} = 460 nm and λ_{emi} = 610 nm) the emission from the dimer is favored. Therefore, the shorter lifetime is assigned to the monomer species and the longer one to the dimer species. The latter assignation was performed according to what is already known for $(AOBH^+)_2$ behavior in water [7].

We want to highlight that, for the first time it was possible to characterize the $AOBH^+$ chromophore in solvents of null or very low polarity, such as *n*-heptane and benzene, because, the commercial chloride salt is not soluble in such media.

In *n*-heptane/AOT/water RMs media, the lifetime distribution was performed at two water content: W_0 = 0 and 10 and, at three different AOT concentrations. The results are gathered in Table 3. To explain the results, it must be recalled that, in RMs media there is more than one solubilization site where the species can exist.

For [AOT]<cmc, 5×10^{-5} M, at W_0 = 0 and 10 exciting at λ_{exc} = 460 nm, a bimodal distribution is observed yielding a short lifetime τ = 4.70 ± 0.90 ns and τ = 4.80 ± 0.80 ns and a long lifetime τ = 15.00 ± 2.00 ns and τ = 28.50 ± 0.80 ns, respectively. The shorter lifetime was assigned to monomer species located at the *n*-heptane phase, while the longer lifetime was assigned to the dimer. Exciting at λ_{exc} = 495 nm a unique distribution is observed with an average lifetime of τ = 4.60 ± 0.70 ns and τ = 4.90 ± 0.90 ns for W_0 = 0 and 10 respectively, that also corresponds to the monomer species in the non-polar phase.

For [AOT]>cmc, 5×10^{-3} M, at W_0 = 0, when excited at λ_{exc} = 495 nm (the emission of monomer is favored) a single distribution is observed, with a lifetime equal to τ = 4.00 ± 1.00 ns. This value is comparable to the lifetime value obtained for the monomer in *n*-heptane, therefore it was assigned to this species in the non-polar phase. However, when excited at λ_{exc} = 460 nm (emission from the monomer and dimer species), a bimodal distribution is observed, whit a shorter lifetime of τ = 4.00 ± 1.00 ns which corresponds to the monomer species in the non-polar phase

Table 2
Parameters obtained from the lifetimes distribution analysis of AOBH-DEHP molecule in homogeneous media.

	λ_{exc} (nm)	λ_{emi} (nm)	τ_1/ns	RW%	Species	τ_2/ns	RW%	Species
water	460	527	1.67 ± 0.18	100	monomer			
		610	1.70 ± 0.10	100	monomer			
n-heptane	495	527	4.60 ± 0.70	100				
	460	610	4.00 ± 1.00	93.5	monomer	15.10 ± 2.00	6.5	dimer
benzene	460	533	4.30 ± 0.60	100	monomer			

RW% = relative weight.

Table 3
Parameters obtained from the lifetimes distribution analysis of AOBH-DEHP molecule in *n*-heptane/AOT/water RMs.

[AOT]/M	W_0	λ_{exc} (nm)	λ_{emi} (nm)	τ_1/ns	RW_1%	Species	τ_2/ns	RW_2%	Species
5×10^{-5}	0	495	527	4.60 ± 0.70	100				
		460	610	4.70 ± 0.90	93.5	monomer	15.00 ± 2.00	6.5	dimer
	10	495	530	4.90 ± 0.90	100	monomer			
		460	533	4.80 ± 0.80	92.02	monomer	28.50 ± 0.80	7.98	dimer
5×10^{-3}	0	495	540	4.00 ± 1.00	100	monomer			
		460	543	4.00 ± 1.00	89.07	monomer	14.00 ± 2.00	10.93	monomer
	10	495	545	1.02 ± 0.08	16.43	monomer/H_2O	2.50 ± 0.30	83.57	monomer/RM
		460	545	2.30 ± 0.30	81.05	monomer/RM	4.60 ± 0.30	18.95	monomer/Hp
3×10^{-1}	0	495	537	2.40 ± 0.80	100	monomer			
		460	537	2.30 ± 0.90	100	monomer			
	10	495	543	1.05 ± 0.07	14.65	monomer	2.40 ± 0.20	85.35	monomer
		460	543	0.70 ± 0.10	10.81	monomer	2.40 ± 0.30	86.28	monomer

RM = Reverse Micelle, Hp = *n*-heptane, RW% = relative weight.

and, a longer one of $\tau = 14.00 \pm 2.00$ ns that corresponds to the dimer species in *n*-heptane. At $W_0 = 10$, when excited at $\lambda_{exc} = 460$ nm a bimodal distribution is observed. The longer lifetime, $\tau = 4.60 \pm 0.30$ ns was assigned to monomer species in the non-polar phase. The shorter lifetime of $\tau = 2.30 \pm 0.30$ ns was assigned to the monomer species at the AOT RMs interface, because it resembles the value for $AOBH^+$ at the AOT RMs interface showed before [7]. Interesting, there is no emission from the dimer species coming from the RMs media. It seems that, as discussed before, the RMs favors the disaggregation process of the dye. When excited at $\lambda_{exc} = 495$ nm, a bimodal distribution was observed, with two lifetimes. The short lifetime of $\tau = 1.02 \pm 0.08$ nm was assigned to the monomer species in the aqueous pool of the RMs, while the long lifetime of $\tau = 2.50 \pm 0.30$ nm was assigned to the monomer species that exists at the RMs interface.

For [AOT] = 0.30 M, at $W_0 = 0$, exciting at $\lambda_{exc} = 460$ nm and $\lambda_{exc} = 495$ nm a single distribution is obtained in both cases, with lifetimes values of $\tau = 2.30 \pm 0.90$ ns and $\tau = 2.40 \pm 0.80$ ns, respectively. Those are assigned to the monomer species at the RMs interface. At $W_0 = 10$ exciting at $\lambda_{exc} = 460$ nm and $\lambda_{exc} = 495$ nm, a bimodal distribution is observed. The shorter lifetime $\tau = 0.70 \pm 0.10$ ns and $\tau = 1.05 \pm 0.07$ ns respectively is assigned to the monomer species in the water pool of the RMs, because this value is comparable to the one obtained for the monomer in pure water. The longer lifetime, $\tau = 2.40 \pm 0.30$ nm and $\tau = 2.40 \pm 0.20$ respectively is assigned to the monomer species that exists at the RMs interface.

4. Conclusions

Studies in homogeneous media show that AOBH-DEHP molecule in water and *n*-heptane exists as a monomer and an aggregated species, while in benzene does not. It is demonstrated that the aggregate species in *n*-heptane corresponds to a dimer. The lifetime distribution analysis confirms the presence of these two species. On the other hand, in water the aggregate species is a higher order than a dimer and it is non-fluorescent. A single lifetime value is obtained from the lifetime distribution analysis. In benzene, only the monomer species exists.

In benzene/AOT/water RMs at both $W_0 = 0$ and 10, a single band in the absorption and emission spectra is observed, and they do not change increasing the surfactant concentration. This indicates that AOBH-DEHP molecule is not confined within the RMs media and, it is solubilized in the organic phase (benzene), as monomer.

In *n*-heptane/AOT/water RMs it is observed the disaggregating effect that the RMs has on AOBH-DEHP molecule. As the AOT concentration increases, the monomer species becomes the predominant. This phenomenon is of great importance since it allows to determine the cmc value of RMs.

The REES experiments in *n*-heptane/AOT/water RMs show that AOBH-DEHP detects a restricted motion environment. The REES value drops from 9 nm at $W_0 = 0$–4 nm at $W_0 = 10$.

Finally, it was demonstrated that AOBH-DEHP is a unique protic ionic liquid that can be used as molecular probe to investigate the microenvironments of confined media.

Acknowledgements

Financial support from the Consejo Nacional de Investigaciones Científicas y Técnicas (CONICET, PIP CONICET 112-201101-00204), Universidad Nacional de Río Cuarto, Agencia Nacional de Promoción Científica y Técnica (PICT 2012-0232), and Ministerio de Ciencia y Tecnología, Gobierno de la Provincia de Córdoba (PID-2013) is gratefully acknowledged. N.M.C., J.J.S. and R.D.F. hold a research position at CONICET. M.A.C. thanks CONICET for a research fellowship.

Appendix A. Supplementary data

Supplementary data related to this article can be found at http://dx.doi.org/10.1016/j.dyepig.2016.11.031.

References

[1] Steed JW, Turner DR, Wallace KJ. Core concepts. In: Supramolecular chemistry and nanochemistry. John Wiley & Sons; 2007.
[2] Cosgrove T, editor. Colloid science principles, methods and applications. 2 ed. John Wiley & Sons; 2010.
[3] Fanun M, editor. Microemulsions: properties and applications. CRC Press, Taylor & Francis Group; 2009.
[4] Vriezema DM, Aragonès MC, Elemans JAAW, Cornelissen JJLM, Rowan AE, Nolte RJM. Self-assembled nanoreactors. Chem Rev 2005;105:1445–90.
[5] Silber JJ, Biasutti MA, Abuin E, Lissi E. Interactions of small molecules with reverse micelles. Adv Colloid Interface Sci 1999;82:189–252.
[6] Moulik SP, Paul BK. Structure, dynamics and transport properties of microemulsions. Adv Colloid Interface Sci 1998;78:99–195.
[7] Falcone RD, Correa NM, Biasutti MA, Silber JJ. Acid–Base and aggregation processes of acridine orange base in *n*-heptane/AOT/water reverse micelles. Langmuir 2002;18:2039–47.
[8] Shinoda K. The significance and characteristics of organized solutions. J Phys Chem 1985;89:2429–31.
[9] Georges J. Molecular fluorescence in micelles and microemulsions: micellar effects and analytical applications. Spectrochim Acta Rev 1990;13:27–45.
[10] Djeghaba Z, Deleuze H, Dejeso B, Messadi D, Maillard B. Enzymes in organic synthesis VII: enzymatic acylation of amines. Tetrahedron Lett 1991;32(6):761–2.
[11] Azuma N, Furuuchi S, Takahara H, Sugawara K, Kanno C. Electron microscopic study on the influence of deimination on casein micelle formation. J Diary Sci 1998;81:64–8.
[12] Moyano F, Setien E, Silber JJ, Correa NM. Enzymatic hydrolysis of N-Benzoyl-l-Tyrosine p-nitroanilide by α-chymotrypsin in DMSO-water/AOT/n-heptane reverse micelles. A unique interfacial effect on the enzymatic activity. Langmuir 2013;29:8245–54.
[13] Blach D, Silber JJ, Correa NM, Falcone RD. Electron donor ionic liquids entrapped in anionic and cationic reverse micelles. Effects of the interface on the ionic liquid–surfactant interactions. Phys Chem Chem Phys 2013;15:16746–57.
[14] Correa NM, Biasutti MA, Silber JJ. Micropolarity of reverse micelles of aerosol-OT in *n*-hexane. J Colloid Interface Sci 1995;172:71–6.
[15] Falcone RD, Silber JJ, Correa NM. What are the factors that control non-aqueous/AOT/*n*-heptane reverse micelle sizes? A dynamic light scattering study. Phys Chem Chem Phys 2009;11:11096–100.
[16] Grand D. Electron transfer in reverse micellar Solutions: influence of the interfacial bound water. J Phys Chem B 1998;102:4322–6.
[17] Quintana SS, Moyano F, Falcone RD, Silber JJ, Correa NM. Characterization of multifunctional reverse micelles' interfaces using hemicyanines as molecular probes. II: effect of the surfactant. J Phys Chem B 2009;113:6718–24.
[18] Moyano F, Falcone RD, Mejuto CJ, Silber JJ, Correa NM. Cationic reverse micelles create water with super hydrogen-bond-donor capacity for enzymatic catalysis: hydrolysis of 2-Naphthyl acetate by α-chymotrypsin. Chem.-Eur J 2010;16:8887–93.
[19] Agazzi FM, Falcone RD, Silber JJ, Correa NM. Solvent blends can control cationic reversed micellar interdroplet interactions. the effect of *n*-Heptane: benzene mixture on BHDC reversed micellar interfacial properties: droplet sizes and micropolarity. J Phys Chem B 2011;115:12076–84.
[20] Gutierrez JA, Falcone RD, Silber JJ, Correa NM. C343 behavior in benzene/AOT reverse micelles. The role of the dye solubilization in the non-polar organic pseudophase. Dyes Pigm 2012;95:290–5.
[21] Correa NM, Silber JJ, Riter RE, Levinger NE. Nonaqueous polar solvents in reverse micelle systems. Chem Rev 2012;112:4569–602.
[22] Quintana SS, Falcone RD, Silber JJ, Correa NM. Comparison between two anionic reverse micelle interfaces: the role of water–surfactant interactions in interfacial Properties. ChemPhysChem 2012;13:115–23.
[23] El Seoud OA, Okano LT, Novaki LP, Barlow GK. Ber. *Bunsenges.* Proton NMR studies on the structure of water in ionic and nonionic water-in-oil microemulsions. Phys Chem 1996;100:1147–52.
[24] Novaki LP, El Seoud OA, Lopes JCD. Ber. *Bunsenges.* An FT-IR study on the structure of water solubilized by cetyltrimethylammonium bromide reverse aggregates in chloroform/*n*-Dodecane. Phys Chem 1997;101:1928–32.
[25] Novaki LP, El Seoud OA. A fourier transform infrared study on the structure of water solubilized by reverse aggregates of sodium and magnesium Bis(2-ethylhexyl)sulfosuccinates in organic solvents. J Colloid Interface Sci 1998;202:391–8.
[26] De TK, Maitra A. Solution behaviour of aerosol OT in non-polar solvents. Adv Colloid Interface Sci 1995;59:95–193.
[27] Moulik SP, Paul BK. Structure, dynamics and transport properties of microemulsions. Adv Colloid Interface Sci 1998;1998(78):99–195.
[28] Correa NM, Levinger NE. What can you learn from a molecular Probe? New insights on the behavior of C343 in homogeneous solutions and AOT reverse micelles. J Phys Chem B 2006;110:13050–61.

[29] Novaira N, Biasutti MA, Silber JJ, Correa NM. New Insights on the photophysical behavior of PRODAN in anionic and cationic reverse micelles: from which state or states does it emit? J Phys Chem B 2007;111:748–59.
[30] Feng X-Z, Lin Z, Yang L-J, Wang C, Bai C-L. Investigation of the interaction between acridine orange and bovine serum albumin. Talanta 1998;47:1223–9.
[31] See for example: a) Zimmermann F, Hossenfelder B, Panitz J-C, Wokaun A. SERRS study of acridine orange and its binding to DNA strands. J Phys Chem 1994;98:12796–804.
b) Brauns EB, Murphy CJ, Berg MA. Local dynamics in DNA by temperature-dependent stokes shifts of an intercalated dye. J Am Chem Soc 1998;120:2449–56.
c) Davies DB, Veselkov DA, Kodintsev VV, Evstigneev MP, Veselkov AN. 'H NMR investigation of the hetero-association of aromatic molecules in aqueous solution: factors involved in the stabilization of complexes of daunomycin and acridine drugs. Mol Phys 2000;98:1961–71.
[32] Gupta S, Mukhopadhyay L. Behaviour of acridine orange in aqueous and in water/AOT/decane w/o microemulsion medium in presence of additives. Indian J Chem 1997;36A:31–7.
[33] Ortona O, Vitagliano V, Robinson BH. Dye interactions with surfactants in colloidal dispersions. J Colloid Interface Sci 1988;125:271–8.
[34] Falcone RD, Correa NM, Biasutti MA, Silber JJ. The use of acridine orange base (AOB) as molecular probe to characterize nonaqueous AOT reverse micelles. J Colloid Interface Sci 2006;296:356–64.
[35] Hallett JP, Welton T. Room-temperature ionic liquids: solvents for synthesis and catalysis 2. Chem Rev 2011;111:3508–76.
[36] Welton T, Wasserscheid P. Ionic liquids in synthesis. Weinheim: VCH-Wiley; 2002.
[37] Welton T. Ionic liquids in catalysis. Coord Chem Rev 2004;248:2459–77.
[38] Angell CA, Byrne N, Belieres JP. Parallel developments in aprotic and protic ionic liquids: physical chemistry and applications. Acc Chem Res 2007;40:1228–36.
[39] a) Pernak J, Goc I, Mirska I. Anti-microbial activities of protic ionic liquids with lactate anion. Green Chem 2004;66:323–9.
b) Hangarge RV, Jarikote DV, Shingare MS. Knoevenagel condensation reactions in an ionic liquid. Green Chem 2002;4:266–8.
c) Laali KK, Gettwert VJ. Electrophilic nitration of aromatics in ionic liquid solvents. J Org Chem 2001;66:35–40.
d) Hu Y, Chen J, Le Z, Zheng QG. Organic reactions in ionic liquids: ionic liquids ethylammonium nitrate promoted knoevenagel condensation of aromatic aldehydes with active methylene compounds. Synth Commun 2005;35:739–44.
e) Poole CF. Chromatographic and spectroscopic methods for the determination of solvent properties of room temperature ionic liquids. J Chromatogr A 2004;1037:49–82.
f) Susan A B H Md, Noda A, Mitushima S, Watanabe M. Brønsted acid–base ionic liquids and their use as new materials for anhydrous proton conductors. Chem Commun 2003:938–9.
g) Araos MU, Warr GG. Self-assembly of nonionic surfactants into lyotropic liquid crystals in ethylammonium nitrate, a room-temperature ionic liquid. J Phys Chem B 2005;109:14275–7.
h) Atkin R, Warr GG. Self-assembly of a nonionic surfactant at the graphite/ionic liquid interface. J Am Chem Soc 2005;127:11940–1.
i) Picquet M, Tkatchenko I, Tommasi I, Wasserscheid P, Zimmermann J. Ionic liquids, 3. Synthesis and utilisation of protic imidazolium salts in homogeneous catalysis. Adv Synth Catal 2003;345:959–62.
[40] Hayes R, Imberti S, Warr GG, Atkin R. Effect of cation alkyl chain length and anion type on protic ionic liquid nanostructure. J Phys Chem C 2014;118:13998–4008.
[41] Quintana SS, Falcone RD, Silber JJ, Correa NM, Moyano F. On the characterization of NaDEHP/n-heptane nonaqueous reverse micelles: the effect of the polar solvent. Phys Chem Chem Phys 2015;17:7002–11.
[42] Ueda M, Schelly ZA. Reverse micelles of Aerosol-OT in benzene. 4. Investigation of the micropolarity using 1-methyl-8-oxyquinolinium betaine as a probe. Langmuir 1989;5:1005–8.
[43] O'Connor DV, Phillips D. In: Academic Press, editor. Time-correlated single photon counting. New York: E-Publishing Inc; 1983. p. 158–97.
[44] Siemiarczuk A, Wagner BD, Ware WR. Comparison of the maximum entropy and exponential series methods for the recovery of distributions of lifetimes from fluorescence lifetime data. J Phys Chem 1990;94:1661–6.
[45] El-Kemary MA, El-Mehasseb IM. Global and distribution analysis of fluorescence decays and spectrofluorimetric determination of stoichiometry and association constant of the inclusion complex of 2-amino-5,6-dimethylbenzimidazole with β-cyclodextrin. Talanta 2004;62:317–22.
[46] Malicka J, Ganzynkowicz R, Groth M, Czaplewski C, Karolczak J, Liwo A, et al. Fluorescence decay time distribution analysis of cyclic enkephalin analogues; Influence of solvent and Leu configuration in position 5 on conformation. Acta Biochim Pol 2001;48:95–102.
[47] a) Maiti NC, Mazumdar S, Periasamy N. J- and H-Aggregates of Porphyrin–Surfactant complexes: time-resolved fluorescence and other spectroscopic studies. J Phys Chem B 1998;102:1528–38.
b) Togashi DM, Costa SMB, Sobral AJFN, Gonsalves A M d'A R. Self-aggregation of lipophilic porphyrins in reverse micelles of aerosol OT. J Phys Chem B 2004;108:11344–56.
c) Molina PG, Silber JJ, Correa NM, Sereno L. Electrochemistry in AOT reverse micelles. A powerful technique to characterize organized media. J Phys Chem C 2007;111:4269–76.
[48] Lang J, Jada A, Malliaris A. Structure and dynamics of water-in-oil droplets stabilized by sodium bis(2-ethylhexyl) sulfosuccinate. J Phys Chem 1988;92:1946–53.
[49] Kelkar DA, Chattopadhyay A. Depth-Dependent solvent relaxation in reverse Micelles: A fluorescence approach. J Phys Chem B 2004;108:12151–8.
[50] Lakowicz JR. Principles of fluorescence spectroscopy. second ed. New York: Kluwer; 1999.
[51] Moyano F, Silber JJ, Correa NM. On the investigation of the bilayer of large unilamellar vesicles using different cationic hemicyanines and DPH. a wavelenght – selective fluorescense approach. J Colloid Interface Sci 2008;317:332–45.